Electronic Supplementary Material (ESI) for RSC Advances.

Supporting Information

An Anode Buffer Layer with Size-Controlled Ag Nanoparticles for Polymer Solar Cells with Improved Efficiencies

Dhanavel Ganeshan[a, b], Shan-Ci Chen[a], Zhigang Yin[a, b], Qingdong Zheng*[a]

[a] State Key Laboratory of Structural Chemistry, Fujian Institute of Research on the Structure of Matter, Chinese Academy of Sciences, 155 Yangqiao West Road, Fuzhou, Fujian 350002, P. R. China
[b] University of Chinese Academy of Sciences, Beijing 100049, P. R. China

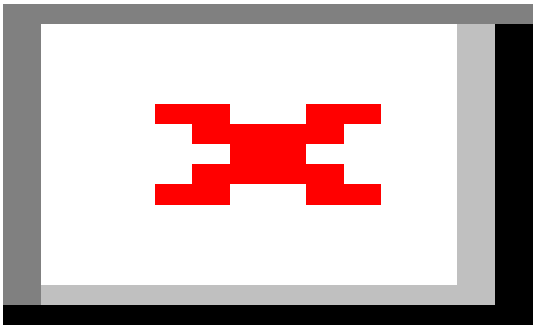

Fig. S1 (a) UV–vis spectra of Ag NPs with the average size of 4 nm; the insets present a picture of the Ag NPs solution and a TEM image of the Ag NPs (4 nm). Scale bar: 100 nm. (b) HRTEM image of the Ag NPs (10 nm) shown in panel a. Scale bar: 5 nm.

Figure S1 illustrates the silver nanoparticles (Ag NPs) prepared by the sodium borohydride ($NaBH_4$) reduction of silver nitrate ($AgNO_3$) in the presence of concentrated citrate at 70°C (experiment section for more details). TEM image shows that these spherical Ag NPs have narrow size distribution at 4±0.9 nm. The sharp extinction at 395 nm and the bright yellowish

solution manifest the characteristic feature from localized surface plasmon resonance (LSPR) of the Ag NPs.[1]

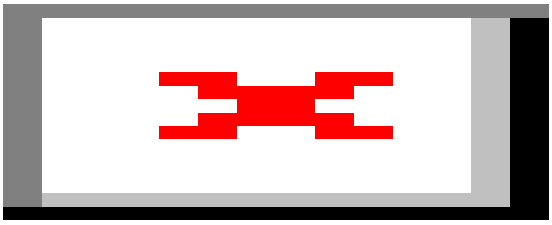

Fig. S2 SEM images of the quasi-spherical Ag NPs with different sizes: (a) 28 nm; (b) 55 nm; (c) 75 nm.

Figure S2 illustrates scanning electron microscopy (SEM) images and size distribution histograms of the fabricated Ag NPs. The dimensions were analyzed directly from SEM images.

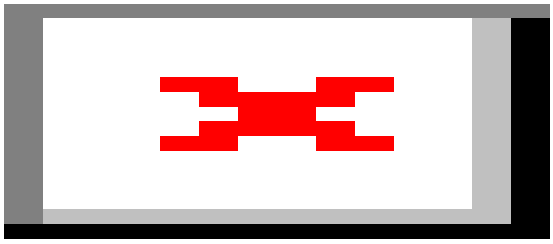

Fig. S3 Typical (a) TEM images 55 nm size of Ag NPs. (b) HRTEM images of the quasi-spherical Ag NPs shown in panel a. Scale bar: 5 nm, and (c) corresponding SAED pattern taken from a single Ag NP.

Figure S3 illustrates the typical transmission electron microscopy (TEM) and high-resolution transmission electron microscopy (HR-TEM) images for the as-transformed product,

respectively, confirming the interplanar crystal spacing of the Ag NPs. A selected area electron diffraction (SAED) was used to confirm the high crystallinity of the synthesized single NP.[2] PSCs with the average diameter of 55 nm exhibit the best performance, so we verified the origin of particle size by using a field emission transmission electron microscope (FEI Tecnai, G[2] F-20 S-TWIN) operated at 200kV, respectively.

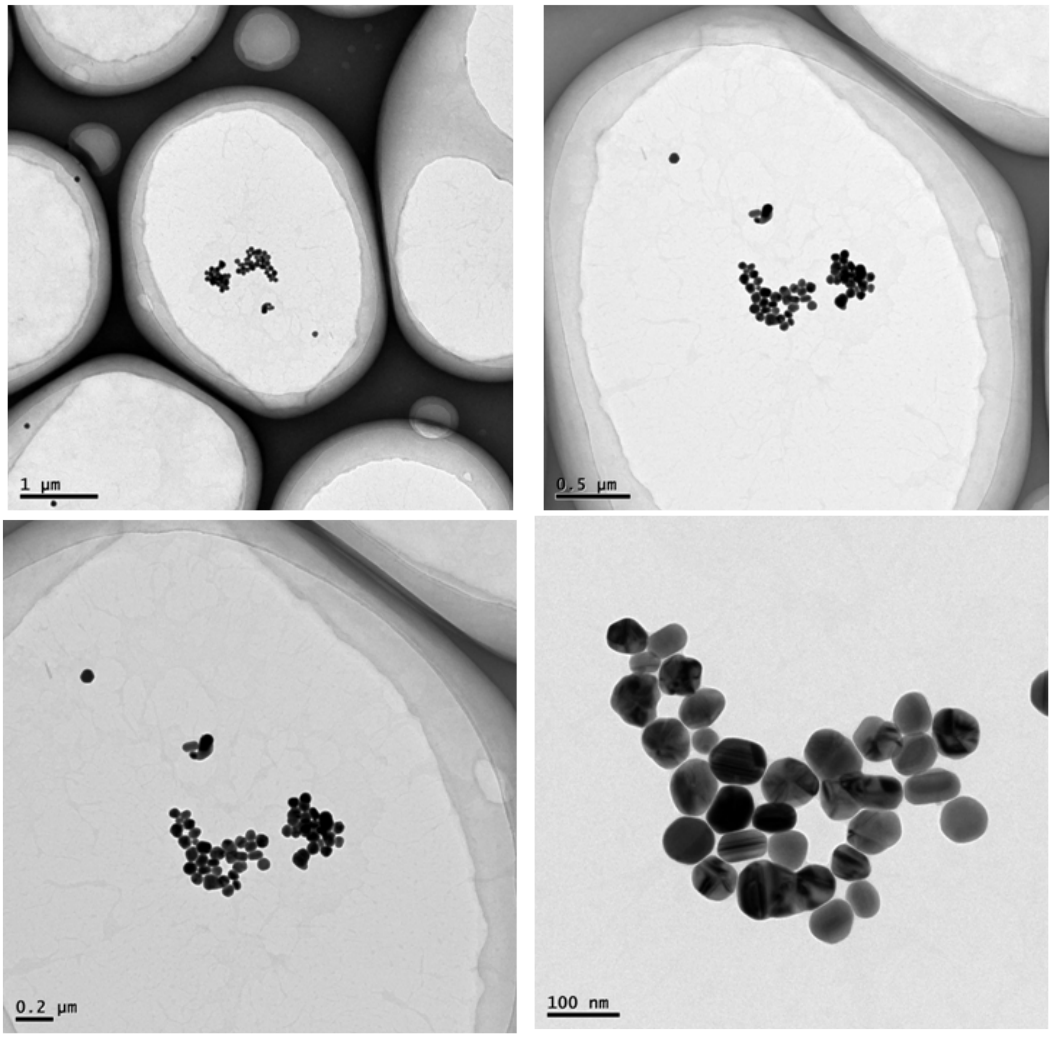

Fig. S4 Plane-view bright field TEM images of 55 nm size of Ag NPs (different scales) embedded in a PEDOT:PSS solution with a concentration of (5:1, w/w).

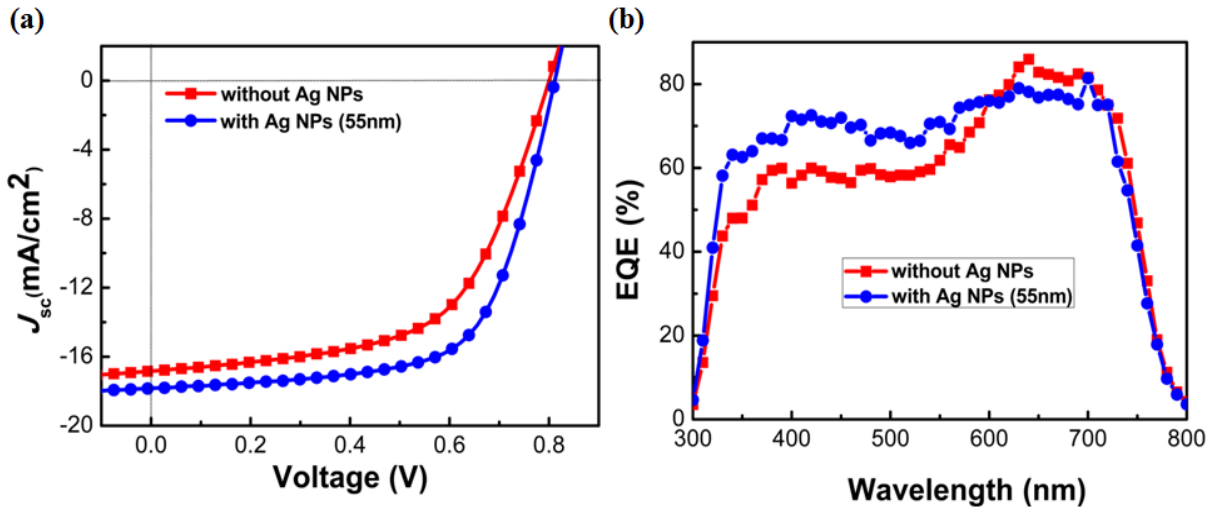

Fig. S5 The best results of *J-V* and EQE characteristics of solar cells with 55 nm Ag NPs and without Ag NPs. (a) The *J-V* curves of the best plasmonic PSC (blue circles) and the control device (red squares). (b) The EQE characteristics of a plasmonic PSC (blue circles) and a control device (red squares) of PTB7-Th:$PC_{71}BM$.

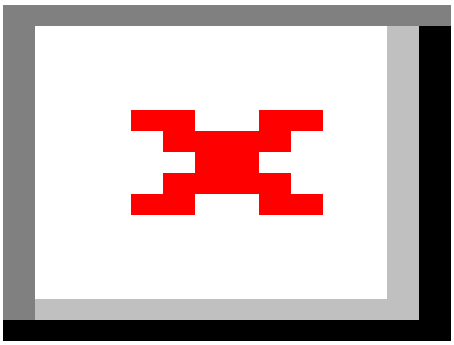

Fig. S6 AFM 3D height images for ITO/PEDOT:PSS films with/without various sized Ag NPs: (a) control device, (b) 4 nm, (c) 28 nm, (d) 55nm, and (e) 75 nm. The corresponding mean roughnesses (RMS) of these films are 0.948 nm, 0.968 nm, 1.006 nm, 1.027 nm, and 1.246 nm, respectively.

Table S1 The measured current densities and calculated current densities from external quantum efficiency measurement.

Devices	J_{sc} (J-V) [mA/cm^2]	J_{sc} (EQE) [mA/cm^2]	Error [%]
Control device	16.81	16.78	0.2
Ag NPs (4 nm)	17.47	16.82	3.7
Ag NPs (28 nm)	17.65	16.98	3.8
Ag NPs (55 nm)	17.82	17.48	1.9
Ag NPs (75 nm)	18.07	17.94	0.7

References:

1. Y. Wan, Z. Guo, X. Jiang, K. Fang, X. Lu, Y. Zhang and N. Gu, *J. Colloid Interface Sci.*, 2013, **394**, 263-268.
2. S. Agnihotri, S. Mukherji and S. Mukherji, *RSC Advances*, 2014, **4**, 3974-3983.